American Mineralogist, Volume 78, pages 988–1001, 1993

O isotope zoning in garnet and staurolite: Evidence for closed-system mineral growth during regional metamorphism

MATTHEW J. KOHN, JOHN W. VALLEY, DON ELSENHEIMER,* MICHAEL J. SPICUZZA
Department of Geology and Geophysics, University of Wisconsin–Madison, Madison, Wisconsin 53706, U.S.A.

ABSTRACT

Microanalysis of O isotope ratios has been made in traverses across two garnet crystals and one staurolite sample (all ~1 cm in diameter) from a metapelitic schist and across one garnet sample ~4.5 mm in diameter from an amphibolite from the Cordillera Darwin metamorphic complex, Tierra del Fuego, Chile. The metapelitic sample contains garnet + biotite + staurolite + plagioclase + muscovite + quartz + ilmenite + chlorite, and *P-T* conditions determined from mineral rims were approximately 575 °C and 7 kbar. O isotope analyses were collected with a spatial resolution of 0.5–1 mm using a laser extraction system. The 72 analyses of the two garnet crystals in the metapelite indicate a gradual increase in $\delta^{18}O$ from ~3.5‰ (V-SMOW) in the core to ~4.0‰ at the rims. The 70 analyses of the staurolite grain show that it is generally unzoned, with an average value of 4.37 ± 0.08‰ (1σ), except for localized increases in $\delta^{18}O$ toward some parts of the rim; these increases may be the result of late chlorite alteration. The garnet amphibolite sample contains garnet + biotite + plagioclase + quartz + chlorite + hornblende + cummingtonite, and *P-T* conditions were approximately 625 °C and 4.5 kbar. The 25 analyses of the garnet sample indicate that it is homogeneous, with an average isotopic value of 3.44 ± 0.05‰ (1σ), except for three analyses that average 3.26‰. The 22 analyses of the fine-grained matrix near the garnet indicate that the matrix is compositionally nearly homogeneous, with an average value of 3.70 ± 0.15‰ (1σ).

With this *P-T-t* path, the reaction history, and no infiltration by a fluid with disequilibrium $\delta^{18}O$, the predicted prograde zonation for the metapelitic garnets is between +0.2 and +0.75‰ (rim to core), with a best estimate of +0.5‰. The zonation for staurolite is ~−0.05‰, and for the amphibolitic garnet it is between −0.01 and +0.06‰. The correspondence of the predictions and observations suggests that the rocks were not infiltrated by a fluid that is not in isotopic equilibrium during regional metamorphism. The data show that regional metamorphic garnet and staurolite can preserve prograde variations of O isotopes in amphibolite facies terranes.

INTRODUCTION

A principal goal of metamorphic petrologists is to determine the degree to which rocks are open or closed to infiltration by a fluid that is out of equilibrium with the rock. Studies demonstrate the power of O isotope analysis for interpreting such metamorphic processes (e.g., see reviews by Rumble, 1982; Valley, 1986; Nabelek, 1991). Prograde O isotope zoning in metamorphic porphyroblasts (e.g., Garlick and Epstein, 1967; Chamberlain and Conrad, 1991; Kohn, 1993) is a potentially sensitive monitor of fluid evolution because the changes of mineral $\delta^{18}O$ for regional metamorphic systems that are closed to fluid infiltration are readily predictable for a given bulk composition, assemblage, and *P-T* history (Kohn, 1993). With analytically and spatially precise analysis of O isotopes, a direct comparison of theory and observation is possible for rocks whose *P-T* and reaction histories are well understood.

We present data on the zoning of O isotopes from regional metamorphic garnet and staurolite porphyroblasts from Cordillera Darwin, Tierra del Fuego, Chile. These results are unique in that (1) no previous study of the zoning of O isotopes has been conducted on regional metamorphic rocks whose *P-T-t* and reaction histories are as well known, and (2) no previous study has obtained such good analytical precision (<±0.1‰, 1σ) and such high analytical densities (up to 25 analyses per 14 mm^2 and 25–70 analyses per mineral grain) using fluorination techniques. The isotopic data, in combination with the well-constrained *P-T-t* path and theoretical models of isotopic zonation, show that these rocks experienced little or no infiltration by an isotopic disequilibrium fluid during regional metamorphism.

GEOLOGIC BACKGROUND

The Cordillera Darwin metamorphic complex, located at the southern tip of South America (Fig. 1), contains greenschist- to upper-amphibolite-grade metamorphic rocks.

* Present address: Geological Survey of Japan, 1-1-3 Higashi, Tsukuba, Ibaraki, 305 Japan.

0003–004X/93/0910–0988$02.00

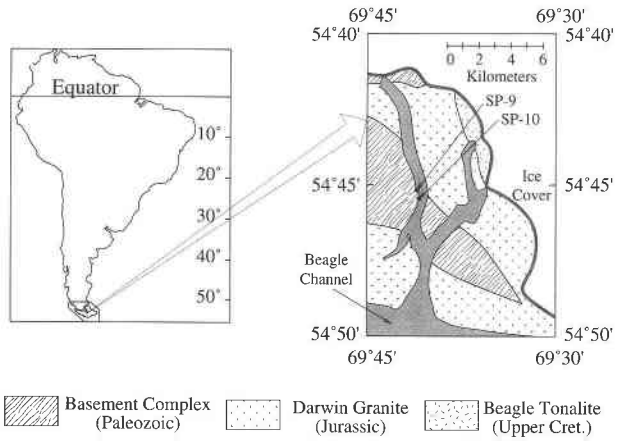

Fig. 1. Map of the Cordillera Darwin area of Tierra del Fuego, showing location of samples SP-9A and SP-10A1. For more detailed geologic, petrologic, and geochronologic data and interpretations, see Nelson et al. (1980), Dalziel and Brown (1989), and Kohn et al. (1991, 1993, and in preparation).

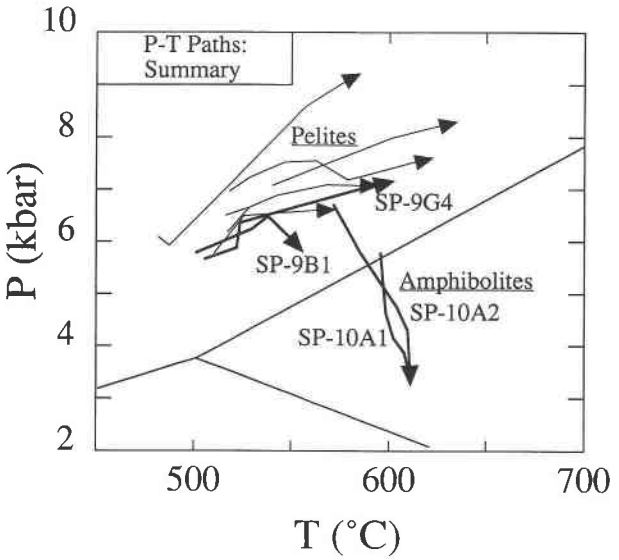

Fig. 2. Plot of pressure-temperature paths calculated for rocks from the Cordillera Darwin metamorphic complex (Kohn et al., 1993). *P-T* paths from metapelitic rocks show garnet growth during an increase in temperature and pressure. *P-T* paths from SP-10A1 and SP-10A2 garnet amphibolites show a decrease in pressure with increasing temperature during garnet growth.

Recent structural and tectonic syntheses have been proposed by Nelson et al. (1980) and Dalziel and Brown (1989), and detailed metamorphic and geochronologic studies have been described by Kohn et al. (1993 and in preparation); the features of this previous work that are salient to the present study are summarized below.

Closure of a marginal basin in the mid-Cretaceous (~100 Ma) resulted in regional metamorphism that reached kyanite grade for the sample locations described in this study. *P-T* paths from the area are shown in Figure 2. The peak *P-T* conditions for the SP-9 outcrop are estimated to have been 575 °C and 7 kbar, and *P-T* path analysis of other metapelitic garnets from that outcrop and those at lower grades suggests that sample SP-9A probably grew garnet in the assemblage garnet + biotite + chlorite + muscovite + quartz + plagioclase + H_2O-rich fluid over an increase in temperature of between 45 and 105 °C and a pressure increase of between 0.25 and 1.25 kbar. Because of their different bulk compositions, the garnet amphibolites (SP-10) record lower rim pressures (3–5 kbar) than the nearby metapelites do, and *P-T* path analysis of sample SP-10A1 indicates that garnet grew in the assemblage garnet + chlorite + biotite + hornblende + cummingtonite + quartz + plagioclase + H_2O-rich fluid over a temperature increase of ~20 °C and a pressure decrease of ~1.5 kbar. The $^{40}Ar/^{39}Ar$ analysis of hornblende, muscovite, biotite, and potassium feldspar from the area indicates rapid cooling from peak metamorphic conditions at rates of ~25 °C/m.y. for these rocks (Kohn et al., 1991 and in preparation).

Petrography and reaction history

Sample SP-9A contains garnet + biotite + muscovite + plagioclase + quartz + staurolite + ilmenite + chlorite. Garnets reach ~1 cm in diameter, are rounded, and contain inclusions of epidote in their cores and ilmenite and quartz throughout. Garnets with ≤5% inclusions were chosen for isotope analysis to minimize potential contamination. Most chlorite in the sample is interpreted to be an alteration phase after staurolite, biotite, or garnet because it occurs in fine-grained mats along grain boundaries and fractures. However, because some matrix chlorite grains are in Fe-Mg-Mn partitioning equilibrium with garnet, biotite, and staurolite (Kohn, 1991; Kohn et al., 1993) and are not spatially associated with other ferromagnesian phases, it is unclear whether all chlorite is retrograde. Idioblastic staurolite porphyroblasts (~1 cm in diameter) cut across the foliation defined by muscovite and biotite, are nearly inclusion-free except for minor ilmenite, pyrrhotite, and quartz (<2%) and occasionally have chlorite alteration along crosscutting fractures. Ilmenite and quartz inclusions in the staurolite tended to be larger than those in the garnet and could be more easily removed mechanically. Quartz and plagioclase are equant and xenoblastic, and they average ~0.25 mm in diameter. Muscovite and biotite flakes are typically ~0.025 and 0.075 mm thick, respectively, and ~0.2 and 0.75 mm in diameter.

In order to model closed system isotopic zonation, the reaction history of each sample must be known in addition to its *P-T* path. Growth of garnet in the metapelites probably occurred in the assemblage garnet + biotite + chlorite + muscovite + plagioclase + quartz + H_2O-rich fluid ± epidote (Kohn et al., 1993). Resorption of garnet and growth of staurolite probably resulted from the continuous reaction garnet + chlorite + muscovite = biotite + staurolite + H_2O in the MnCKFMASH system. There is no evidence for subsequent garnet growth following

this reaction, and the occurrence of possibly prograde chlorite suggests that the staurolite-forming reaction may not have gone to completion.

Sample SP-10A1 contains the matrix assemblage garnet + biotite + plagioclase + quartz + chlorite + hornblende + cummingtonite. There is no evidence for a change of assemblage during or after garnet growth. Garnets are idioblastic, are >99% inclusion-free, and reach ~5 mm in diameter. Books of biotite and chlorite are typically ~0.25 mm wide and 0.05 mm thick. Plagioclase and quartz are equant and xenoblastic and average ~0.05 mm in diameter; individual plagioclase grains are zoned from An_{50} in their cores to An_{68} at their rims (Kohn et al., 1993). Hornblende and cummingtonite are typically ~0.5 mm long and ~0.075 mm in diameter and are compositionally homogeneous.

Analytical techniques

Sample preparation and data collection

Samples were prepared using the thin sawblade technique (Elsenheimer and Valley, 1993). Rocks were first slabbed, and garnet and staurolite crystals that were particularly inclusion-free were identified. Standard thin-section chips containing the crystals and surrounding matrix material were then cut, and the chips were polished and mounted on a glass slide with acetone-soluble, quick-setting cement. A wafer 500–750 μm thick of garnet, staurolite, and matrix material was cut from each chip, the cut surfaces were lightly polished, and glass coverslips were affixed with the same cement. Each crystal was cut into strips 500 μm wide using a slow-speed ultrathin sawblade (kerfs 100–200 μm thick). Because of fractures, the strips would commonly break apart after the cement was dissolved, but reconstruction was readily possible with photo documentation. Prior to analysis, each strip was broken into pieces between 300 and 1000 μm in length and inspected for inclusions and alteration. Each sample piece was then loaded onto a solid block of Ni with holes 2 mm in diameter drilled into it, along with our laboratory standard Gore Mountain garnet.

Crowe et al. (1990) and Elsenheimer and Valley (1992, 1993) have described in detail the laser extraction system and procedures used at the University of Wisconsin for O isotope analysis. They are similar to the system and procedure described by Sharp (1990, 1992). After preparation, samples were pretreated overnight in the sample chamber with 1000 μmol of BrF_5 (~70 torr) to remove H_2O and any traces of organic compounds. Although this pretreatment can leach O from altered feldspars (Elsenheimer and Valley, 1992, 1993); our additional studies indicate that it does not affect the analysis of garnet, staurolite, quartz, biotite, muscovite, unaltered plagioclase, magnetite, ilmenite, diopside, wollastonite, hornblende, corundum, or zircon. Most samples were heated with a defocused CO_2 laser beam ~500 μm in diameter in the presence of ~1000 μmol of BrF_5 from an initial power density of 5×10^6 W/m^2 to a final power density of 4.5×10^7 W/m^2. Three analyses of quartz were made at a single power density of 4.5×10^7 W/m^2. Samples completely reacted within 1–2 min. Sample sizes were typically in the range 5–20 μmol of CO_2 (0.5–2 mg).

An intralaboratory standard (UW Gore Mountain garnet) was analyzed each day prior to analyzing unknowns to correct for any O fractionation within the extraction system. The $\delta^{18}O$ value for our standard was determined relative to the international standards NBS-28 quartz and NBS-30 biotite, as described below. A memory effect occurred in the extraction system prior to September 1, 1992; such that analyses were biased by the $\delta^{18}O$ value of the preceding analysis. The amount of gas required to overcome the memory of a sample that differed by ~14‰ was found to be ~10–20 μmol. Because the differences between samples and the garnet standard were <3‰ in this study and because sample sizes were ~10 μmol, it is likely that memory effects were negligible. Nonetheless, extra pieces of garnet or staurolite from other parts of the sample were analyzed between the standards and samples in order to ensure that the transition from analyzing the standard to analyzing the sample did not bias the first sample analyses. The differences among the sample analyses were too small to have biased each other.

Standardization, corrections, and analytical precision

Table 1[1] summarizes standard analyses that were used to calibrate the garnet standard and to determine yields, reproducibility, and potential effects of sample size on $\delta^{18}O$. These results show that the difference between NBS-28 quartz and our standard Gore Mountain garnet averages about 3.19 ± 0.04‰ (1σ uncertainty in the difference between the mean values); a similar comparison using NBS-30 biotite indicates a difference of −1.40 ± 0.04‰ (1σ). The accepted values for NBS-28 quartz and NBS-30 biotite are 9.6 and 5.1‰ (relative to V-SMOW), and this leads to calibrated values for our garnet standard of 6.41 ± 0.04‰ (vs. quartz) and 6.50 ± 0.04‰ (vs. biotite). From these comparisons, we prefer an average value for the garnet standard of 6.46‰. Yields on weighed pieces of Gore Mountain garnet were all 100% within weighing uncertainties.

In May and June, 1992; we found that the average measured value of the UW Gore Mountain garnet standard varied from day to day and became progressively lighter by as much as 1‰. The exact cause of this shift to lighter values is unclear, but it may have been the result of the accumulation of fluorides and bromides in the cleanup section of the vacuum line. Because the shift was not correlated with sample size, an absolute daily correction of the analyses was made based on the calibrated value of the Gore Mountain garnet standard (6.46‰) and the mean measured value for that day (Ta-

[1] For a copy of Tables 1–3, order Document AM-93-539 from the Business Office, Mineralogical Society of America, 1130 Seventeenth Street NW, Suite 330, Washington, DC 20036, U.S.A. Please remit $5.00 in advance for the microfiche.

bles 1–4). Because the typical standard deviation at this time for a single day's standardization was 0.1–0.15‰ and four to five analyses were collected, the accuracy of the correction is ~0.05–0.1‰ (1σ uncertainty in the mean). Elsenheimer and Valley (1993) collected data on the same extraction line from February to April, 1992; and obtained a similar reproducibility on standards; no day-to-day drift was observed at that time.

In August, 1992; the extraction line was completely dismantled and cleaned, and two cryogenic traps were replaced. Between September 1 and November 14, 1992; reproducibility for all analyses of UW Gore Mountain garnet was significantly better ($1\sigma = \pm 0.07$‰, $n = 79$), and the daily mean was nearly constant (5.92–6.04‰). The standard deviation of ±0.07‰ represents the long-term reproducibility at this time, and the reproducibility on several individual days was somewhat better than this (±0.05–0.06‰). Because of the excellent day-to-day reproducibility, we made a constant correction, based on an average value of 5.99 ± 0.07‰ (1σ; 1σ uncertainty in the mean is ±0.008‰) for 79 UW Gore Mountain garnet standard analyses collected during September. This correction is within a few hundredths of a part per mil of each daily average.

After November 14, 1992; the reproducibility each day remained better than ±0.1‰, but the daily mean for multiple analyses of UW Gore Mountain garnet showed a greater variation (5.91–6.22‰). The slight deterioration in day-to-day reproducibility at this time was presumably the result of the progressive build-up of fluorides and bromides. For these data, a daily correction was made based on the mean measured value of the standards for that day (Table 1, footnotes of Table 4) and the mean calibrated value.

Figure 3 shows no effect on $\delta^{18}O$ for sample sizes ranging from 7 to 40 μmol (0.5–3.2 mg). Therefore, no correction of isotopic composition for sample size was made. We have not detected a mineral-dependent fractionation in the extraction line for the minerals quartz, magnetite, biotite, plagioclase, and pyroxene, and no compositional correction has been made for mineral type. The analytical reproducibility on individual mineral grains was verified with pieces of a single Gore Mountain garnet ($1\sigma = 0.12$–0.16‰) prior to September 1, 1992; as well as with 22 analyses of the SP-10A1 amphibolitic garnet ($1\sigma = 0.05$‰) and 40 analyses of SP-9A-1 staurolite ($1\sigma = 0.08$‰) after September 1, 1992. These tests indicate precisions that are identical to the powder analyses ($1\sigma = 0.05$–0.16‰). To our knowledge, these silicate data are the most precise yet documented for a CO_2 laser system, and they establish the viability of the technique for studying O isotope zoning of 0.2‰ or greater using samples in the milligram to submilligram size range.

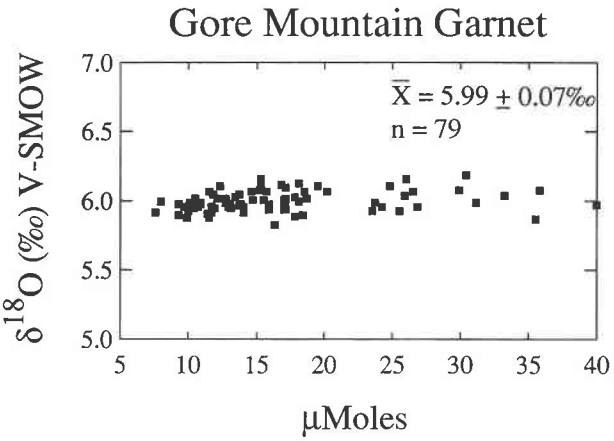

Fig. 3. Plot of 79 analyses from September, 1992, of the University of Wisconsin standard Gore Mountain garnet, showing both excellent reproducibility (±0.07‰, 1σ) and the lack of dependence of measured $\delta^{18}O$ on sample size between ~7 and 40 μmol CO_2 (0.6–3.2 mg).

Comparison of the thin sawblade and in situ techniques

The thin sawblade technique offers substantial advantages over in situ analysis. Firstly, many inclusions can be readily identified and removed if the thin sawblade technique is used but simply must be avoided in in situ analysis. For the staurolite analyzed in this study, large ilmenite and quartz inclusions and minor chlorite alteration along cracks were mechanically removed. If in situ analysis had been used, then 10–20% of the staurolite could not have been analyzed. For cases in which inclusions are small, each mineral fragment can be inspected closely to determine the density of inclusions prior to analysis, and appropriate corrections made. In the metapelitic garnets, the small grain size of ilmenite inclusions precluded their mechanical removal. However, three dimensional inspection of each piece assured us that ilmenite abundance was minor (≤~5%) and uniform. Therefore, any small bias to the garnet analyses (≤~0.2‰) is probably nearly constant for these garnets (≤~±0.05‰). If in situ analysis is used, it is more difficult to determine the three dimensional distribution and abundance of inclusions, especially when they are as platy as ilmenite. Therefore corrections for inclusion abundance have a greater uncertainty.

The subtle zonations documented in this study require high sampling densities of over 100 analyses/cm², and the second advantage of the thin sawblade technique over in situ analysis is that it allows such a high sampling density to be attained. A garnet slab 1 cm in diameter and 500 μm thick contains ~160 mg of material. The saw kerfs remove ~30%, and so ~110 mg of material are analyzable. For an average sample size of 0.5 mg (6 μmol CO_2 for garnet), this results in 220 potential analyses, or a theoretical sampling density of 280 analyses/cm². The results presented in this study document high densities of practical sampling in excess of 100 analyses/cm². For example, in the amphibolite, we extracted 26 pieces of garnet from a single crystal with an area of ~0.14 cm², leading to a density of ~180 analyses/cm². The sampling density for the SP-9A-1 metapelitic garnet was ~120 analyses/cm², and for the staurolite it was ~180 analyses/

TABLE 4. Data for SP-9A and SP-10A1 samples

Date	Analysis no.	$\delta^{18}O$ (‰) raw	$\delta^{18}O$ SMOW	Analysis no.	$\delta^{18}O$ (‰) raw	$\delta^{18}O$ SMOW	Analysis no.	$\delta^{18}O$ (‰) raw	$\delta^{18}O$ SMOW
				SP-10A1 garnet					
9/4/92	3-222-6	3.00	3.47	3-222-7	2.94	3.41	3-222-8	3.04	3.51
9/4/92	3-222-9	2.88	3.35	3-222-10	3.00	3.47	3-222-11	2.91	3.38
9/4/92	3-222-12	2.99	3.46	3-222-13	2.94	3.41	3-222-14	2.89	3.36
9/4/92	3-222-15	2.80	3.27	3-222-16	2.99	3.46	3-222-17	2.91	3.38
9/5/92	3-224-5	3.04	3.51	3-224-6	2.98	3.45	3-224-7	3.04	3.51
9/5/92	3-224-8	3.02	3.49	3-224-9	2.83	3.30	3-224-10	2.74	3.21
9/5/92	3-224-11	—*	—*	3-224-12	2.97	3.44	3-224-13	3.06	3.53
9/5/92	3-224-14	2.99	3.46	3-224-15	3.00	3.47	3-224-16	2.96	3.43
9/5/92	3-224-17	3.04	3.51	3-224-18	2.91	3.38			
				SP-10A1 matrix					
12/9/92	3-274-7	3.70	4.04	3-274-8	3.96	4.30**	3-274-9	3.35	3.69
12/9/92	3-274-10	3.42	3.76						
1/19/93	4-6-6	3.60	3.84	4-6-7	3.64	3.88	4-6-8	3.55	3.79
1/19/93	4-6-9	3.46	3.70	4-6-10	3.27	3.51	4-6-11	3.34	3.58
1/19/93	4-6-12	3.37	3.61	4-6-13	3.21	3.45	4-6-14	3.32	3.56
1/19/93	4-6-15	3.63	3.87	4-6-16	3.32	3.56	4-6-17	3.51	3.75
1/19/93	4-6-18	3.05	3.29†	4-6-19	3.37	3.61	4-6-20	3.54	3.78
1/19/93	4-6-21	3.52	3.76	4-6-22	3.48	3.72	4-6-23	3.22	3.46
				SP-9A-1 garnet					
5/1/92	3-100-7	3.62	4.29	3-100-8	2.96	3.63	3-100-9	2.53	3.20
5/1/92	3-100-10	2.76	3.43	3-100-11	2.99	3.66	3-100-12	2.90	3.57
5/1/92	3-100-13	3.02	3.69	3-100-14	3.25	3.92	3-100-15	3.14	3.81
5/2/92	3-102-8	3.48	3.84	3-102-9	3.66	4.02	3-102-10	3.30	3.66
5/2/92	3-102-11	3.44	3.80	3-102-12	3.08	3.44	3-102-13	3.21	3.57
5/2/92	3-102-14	3.26	3.62	3-102-15	3.52	3.88			
5/3/92	3-104-8	3.44	3.86	3-104-9	3.38	3.80	3-104-10	3.62	4.04
5/3/92	3-104-11	3.34	3.76	3-104-12	3.43	3.85	3-104-13	3.40	3.82
5/3/92	3-104-14	3.23	3.65	3-104-15	3.32	3.74			
9/10/92	3-228-6	3.61	4.08	3-228-7	3.48	3.95	3-228-8	3.27	3.74
9/10/92	3-228-9	3.34	3.81	3-228-10	3.45	3.92	3-228-11	3.39	3.86
9/10/92	3-228-12	3.52	3.99	3-228-13	3.32	3.79	3-228-14	3.45	3.92
9/10/92	3-228-15	3.35	3.82	3-228-16	3.36	3.83	3-228-17	3.36	3.83
2/3/93	4-34-1	3.52	3.90	4-34-2	3.66	4.04	4-34-3	3.53	3.91
2/3/93	4-34-4	3.49	3.87	4-34-5	3.54	3.92	4-34-6	3.37	3.75
2/3/93	4-34-7	3.46	3.84	4-34-8	3.43	3.81	4-34-9	3.46	3.84
2/3/93	4-34-10	3.45	3.83	4-34-11	3.54	3.92	4-34-12	3.38	3.76
2/3/93	4-34-13	3.32	3.70	4-34-14	3.24	3.62	4-34-15	3.12	3.50
2/3/93	4-34-16	3.42	3.80						
				SP-9A-2 garnet					
5/5/92	3-108-6	3.86	4.34	3-108-7	3.53	4.01	3-108-8	3.88	4.36
5/5/92	3-108-9	3.65	4.13	3-108-10	3.60	4.08	3-108-11	3.22	3.70
5/5/92	3-108-12	3.32	3.80	3-108-13	3.22	3.70	3-108-14	3.37	3.85
5/5/92	3-108-15	3.46	3.94	3-108-16	3.24	3.72			
6/13/92	3-122-8	3.34	3.99	3-122-9	3.17	3.82	3-122-10	3.13	3.78
6/13/92	3-122-11	2.98	3.63	3-122-12	3.09	3.74	3-122-13	3.16	3.81
6/13/92	3-122-14	2.86	3.51	3-122-15	2.86	3.51			
				SP-9A-1 staurolite					
6/17/92	3-126-8	4.02	4.82	3-126-9	3.56	4.36	3-126-10	3.94	4.74
6/17/92	3-126-11	3.39	4.19	3-126-12	3.39	4.19	3-126-13	3.76	4.56
6/17/92	3-126-14	3.71	4.51	3-126-15	3.59	4.39	3-126-16	3.66	4.46
6/17/92	3-126-17	3.84	4.64						
6/22/92	3-128-6	3.35	4.54	3-128-7	3.32	4.51	3-128-8	3.61	4.80
6/22/92	3-128-9	3.29	4.48	3-128-10	3.49	4.68	3-128-11	3.43	4.62
6/22/92	3-128-12	3.87	5.06	3-128-13	3.67	4.86	3-128-14	3.82	5.01
6/22/92	3-128-15	3.56	4.75	3-128-16	3.77	4.96			
9/1/92	3-216-6	5.17	5.64	3-216-7	3.90	4.37	3-216-8	3.95	4.42
9/1/92	3-216-9	3.94	4.41	3-216-10	4.72	5.19	3-216-11	4.28	4.75
9/1/92	3-216-12	3.93	4.40	3-216-13	3.86	4.33	3-216-14	3.84	4.31
9/1/92	3-216-15	3.81	4.28	3-216-16	3.94	4.41	3-216-17	3.89	4.36
9/11/92	3-230-7	3.95	4.42	3-230-8	3.87	4.34	3-230-9	3.83	4.30
9/11/92	3-230-10	3.94	4.41	3-230-11	3.78	4.25	3-230-12	3.48	3.95
9/11/92	3-230-13	3.82	4.29	3-230-14	3.81	4.28	3-230-15	3.90	4.37
9/11/92	3-230-16	3.71	4.18						
2/2/93	4-30-10	4.48	4.98	4-30-11	3.87	4.37	4-30-12	3.88	4.38
2/2/93	4-30-13	3.74	4.24	4-30-14	3.90	4.40	4-30-15	3.94	4.44
2/2/93	4-30-16	3.97	4.47	4-30-17	3.84	4.34	4-30-18	3.87	4.37
2/2/93	4-30-19	4.04	4.54	4-30-20	3.76	4.26	4-30-21	3.86	4.36
2/2/93	4-30-22	3.80	4.30	4-30-23	3.85	4.35	4-30-24	3.97	4.47
2/2/93	4-32-1	3.50	4.00‡	4-32-2	3.74	4.24‡	4-32-3	2.84	3.34‡

TABLE 4.—*Continued*

Date	Analysis no.	$\delta^{18}O$ (‰) raw	$\delta^{18}O$ SMOW	Analysis no.	$\delta^{18}O$ (‰) raw	$\delta^{18}O$ SMOW	Analysis no.	$\delta^{18}O$ (‰) raw	$\delta^{18}O$ SMOW
2/2/93	4-32-4	3.91	4.41	4-32-5	3.95	4.45	4-32-6	4.49	4.99
2/2/93	4-32-7	3.89	4.39	4-32-8	3.70	4.20	4-32-9	3.87	4.37
2/2/93	4-32-10	3.95	4.45	4-32-11	3.90	4.40	4-32-12	4.02	4.52
				SP-9A-1 quartz					
2/3/93	4-32-19	7.00	7.38	4-32-20	7.14	7.52	4-32-21	7.60	7.98
				SP-9A-1 plagioclase					
2/3/93	4-32-22	5.44	5.82	4-32-23	5.66	6.04			
				SP-9A-1 muscovite					
5/1/92	3-100-19	4.17	4.84						
5/3/92	3-104-6	4.29	4.72	3-104-7	4.13	4.56			
2/3/93	4-32-24	4.52	4.90						
				SP-9A-2 muscovite					
6/13/92	3-122-6	4.89	5.54						
				SP-9A-1 biotite					
5/2/92	3-102-16	2.59	2.96	3-102-17	2.59	2.96			
5/3/92	3-104-16	3.18	3.61	3-104-17	3.45	3.88			

Note: corrections used were 5/1/92 = 0.67; 5/2/92 = 0.37; 5/3/92 = 0.43; 5/5/92 = 0.48; 6/13/92 = 0.65; 6/17/92 = 0.80; 6/22/92 = 1.19; 9/1/92, 9/4/92, 9/5/92, 9/10/92, and 9/11/92 = 0.47, based on analyses of UW Gore Mountain garnet during September, 1992; 12/9/92 = 0.34; 1/19/92 = 0.24; 2/2/93 = 0.50; 2/3/93 = 0.38. Corrections were based on analyses of UW Gore Mountain garnet (Table 1) prior to sample analysis. Garnets from SP-9A-1 and SP-9A-2 contain ~4% uniformly distributed ilmenite inclusions, so true garnet isotopic composition is ~0.15‰ heavier than indicated in Table 4.

* Analysis lost during transferral.

** Analytical outlier relative to other matrix analyses.

† May have been incompletely reacted.

‡ Contained inclusions of pyrrhotite.

cm^2. In contrast, in situ analysis creates a hole and a surrounding chemical halo that together are as large as ~1 mm in diameter (Crowe et al., 1990; Elsenheimer and Valley, 1992); and this hole weakens the thin wafer during analysis. In practice, the garnets in this study were fractured and would fall apart after 5–10 in situ analyses. Similar results are reported by Chamberlain and Conrad (1991); who collected only 5–10 analyses/cm^2 of garnet. This analytical density is ~20 times smaller than the efficiency we achieved with the thin sawblade technique. For comparison, conventional analysis of 10 mg of material using a Ni vessel would result in a sampling density of 16 analyses/cm^2 for a 500 μm thick wafer.

A final advantage of the thin sawblade technique over in situ analysis is that there are no edge effects that can potentially bias analyses because each mineral fragment is completely reacted. Although we have not made a detailed comparison of the two techniques, data from the literature can be used to evaluate the quality of analysis. Detailed in situ studies of silicates suggest typical reproducibilities of ±0.3–0.4‰ (e.g., Chamberlain and Conrad, 1991; Conrad and Chamberlain, 1992; Elsenheimer and Valley, 1992; Sharp, 1992; Kirschner et al., 1993); whereas the typical reproducibility for this study was ±0.07‰ or better on samples of equivalent size.

RESULTS

Table 4 summarizes analyses of garnet, staurolite, quartz, muscovite, plagioclase, and biotite from samples SP-9A-1 and SP-9A-2 and analyses of the garnet and the matrix of sample SP-10A1. Complete analyses, including standards analyzed, are listed in Tables 1–3. Sketches of the garnets analyzed, locations and $\delta^{18}O$ values of analyses relative to V-SMOW, and compiled zoning profiles are shown in Figures 4 (SP-9A-1) and 5 (SP-10A1). A photomicrograph of the garnet analyzed from sample SP-10A1 also shows the saw cuts used to dissect the sample (Fig. 5). A sketch of the staurolite from sample SP-9A-1 and selected rim-to-rim traverses are shown in Figure 6. All analysis numbers and locations are shown in Figure 7.

Garnet

Contours of $\delta^{18}O$ for the SP-9A-1 garnet were drawn by eye after first making two-point averages of adjacent analyses (Fig. 4A). These contours, in addition to the rim to rim plot of the data for the two central traverses (Fig. 4B), show that the garnet is zoned, with increasing $\delta^{18}O$ from ~3.5‰ in the core to ~4.0‰ on the rim. Because of analytical uncertainties (±0.10‰ or smaller) and the uncertainty in correcting the data for the standard value (±0.05–0.10‰), it is difficult to draw realistic contours for the outer part of the garnet. It may be more systematically zoned than the data suggest. Relative to the rim, the garnet core analyses cannot be biased by ilmenite inclusions because they are so uniformly distributed. The observed zonation cannot be the result of the analysis of epidote inclusions in the core of the garnet because epidote fractionates ^{18}O relative to garnet (e.g., Matthews et al., 1983; Richter and Hoernes, 1988; Kohn and Valley, unpublished data). Correcting for any preferential con-

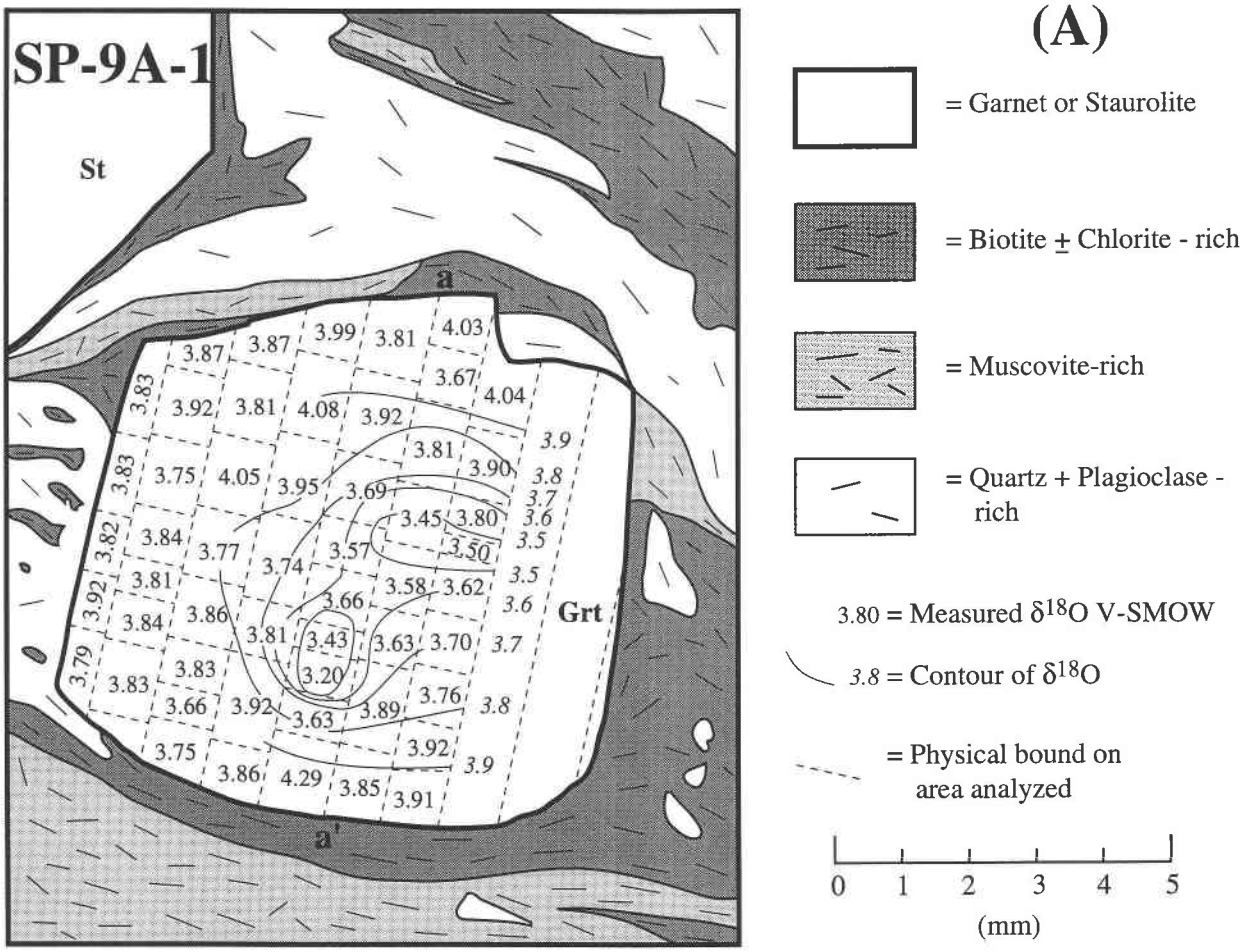

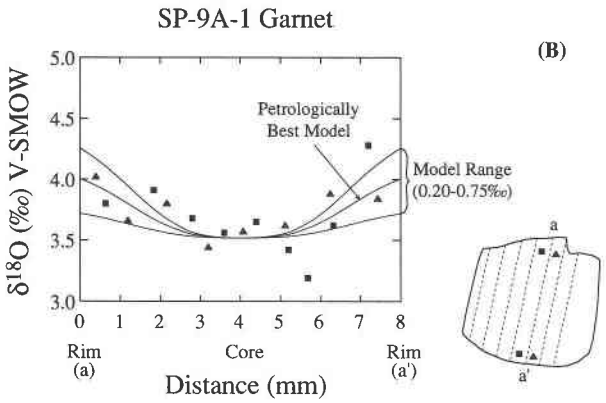

Fig. 4. (**A**) Sketch of garnet from sample SP-9A-1 showing analytical locations, values of analyses, contours of $\delta^{18}O$ V-SMOW, and distribution of matrix minerals. (**B**) Two rim to rim traverses across the center of a garnet from sample SP-9A-1. Right traverse shown by triangles; left traverse shown by squares. Solid lines shows preferred, maximum, and minimum isotopic zoning predicted by theoretical models of closed-system garnet growth (see text).

centration of epidote inclusions in the core would only increase the apparent core to rim O gradient slightly ($\ll$0.1‰). No correction of the garnet isotopic data in Table 4 or Figure 4 was made for ilmenite inclusions. Because the garnet contains ~4% ilmenite inclusions, comparisons of the isotopic fractionations between garnet and other minerals in the rock should include a small constant increase in the $\delta^{18}O$ of garnet of about 0.15‰. The most significant results of this study involve relative differences in intragranular garnet isotopic composition, and so a small constant shift applied to the garnet compositions has no influence on the interpretations presented below.

The data for the SP-10A1 garnet (Fig. 5B and 5C, Table 4) indicate that, with the exception of three analyses, the garnet is remarkably homogeneous, with an average

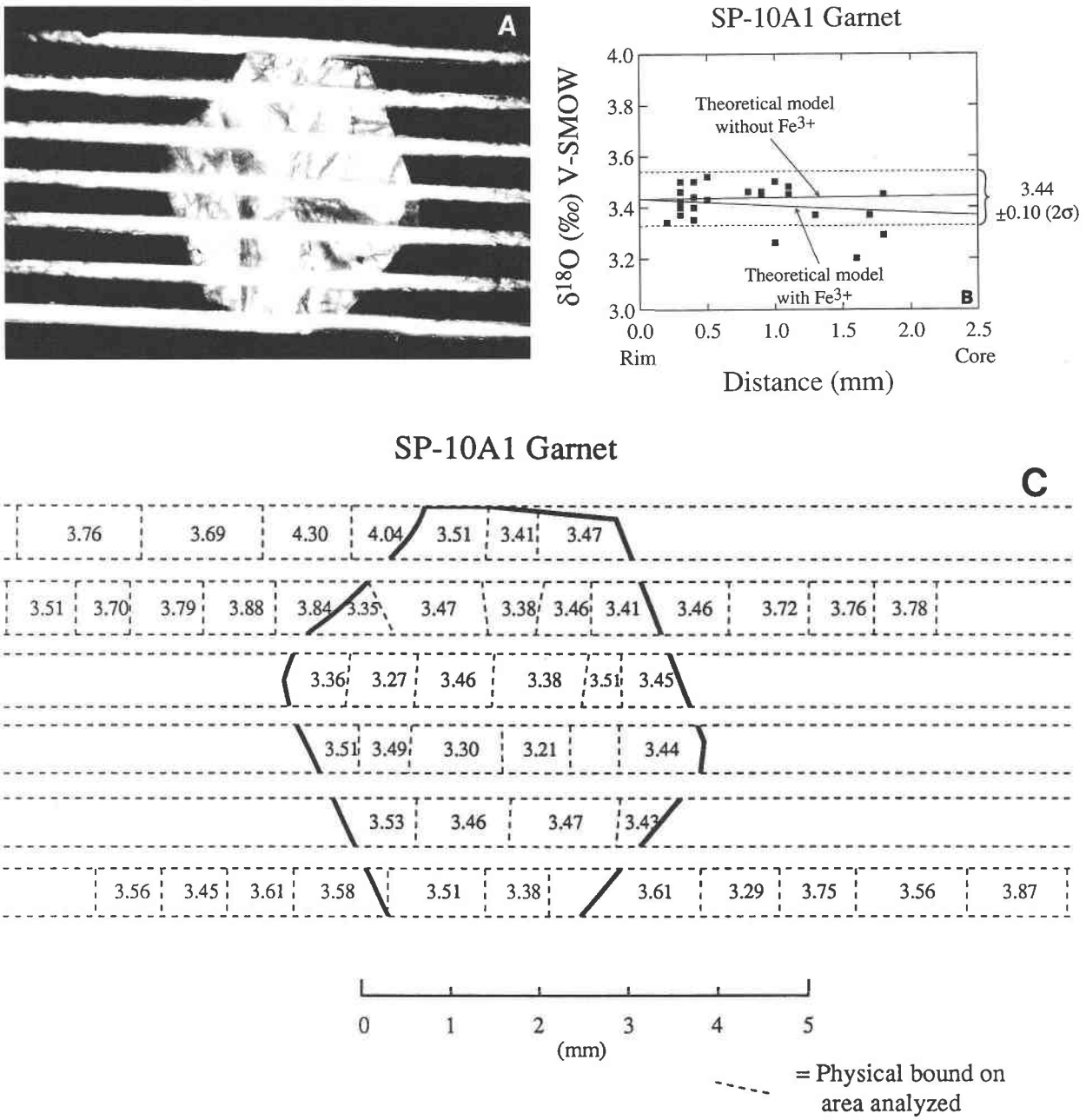

Fig. 5. (A) Photomicrograph of garnet from sample SP-10A1 showing saw cuts used to dissect sample. Garnet is approximately 4.5 mm in diameter. (B) Projection of all analyses onto a core to rim traverse across garnet. Other than three isotopically lighter values (average = 3.26‰) near core, garnet is remarkably homogeneous (3.44 ± 0.05‰, 1σ). Solid lines show maximum and minimum isotopic zoning predicted by theoretical models of closed-system garnet growth. (C) Sketch of garnet from sample SP-10A1 with analytical locations and values. Analyses from outside the garnet are of fine-grained matrix (see text).

$\delta^{18}O$ of 3.44 ± 0.05‰ (1σ). The three analytical outliers are close to the core and are lighter, with values of ~3.26‰. The garnet is ≫99% inclusion free, and so no correction of compositions for inclusions is necessary.

Matrix of SP-10A1

Because the matrix of sample SP-10A1 is fine grained and mineralogically nearly homogeneous, it offers a good opportunity to measure bulk rock O isotopic compositions (minus garnet) and to investigate whether there are any matrix compositional variations that are spatially associated with the garnet porphyroblasts. If we omit two analyses (see footnotes of Table 4), the remaining 20 analyses of the matrix around the garnet are nearly homogeneous, with an average value of 3.70 ± 0.15‰ (1σ). The larger standard deviation for these analyses over the typ-

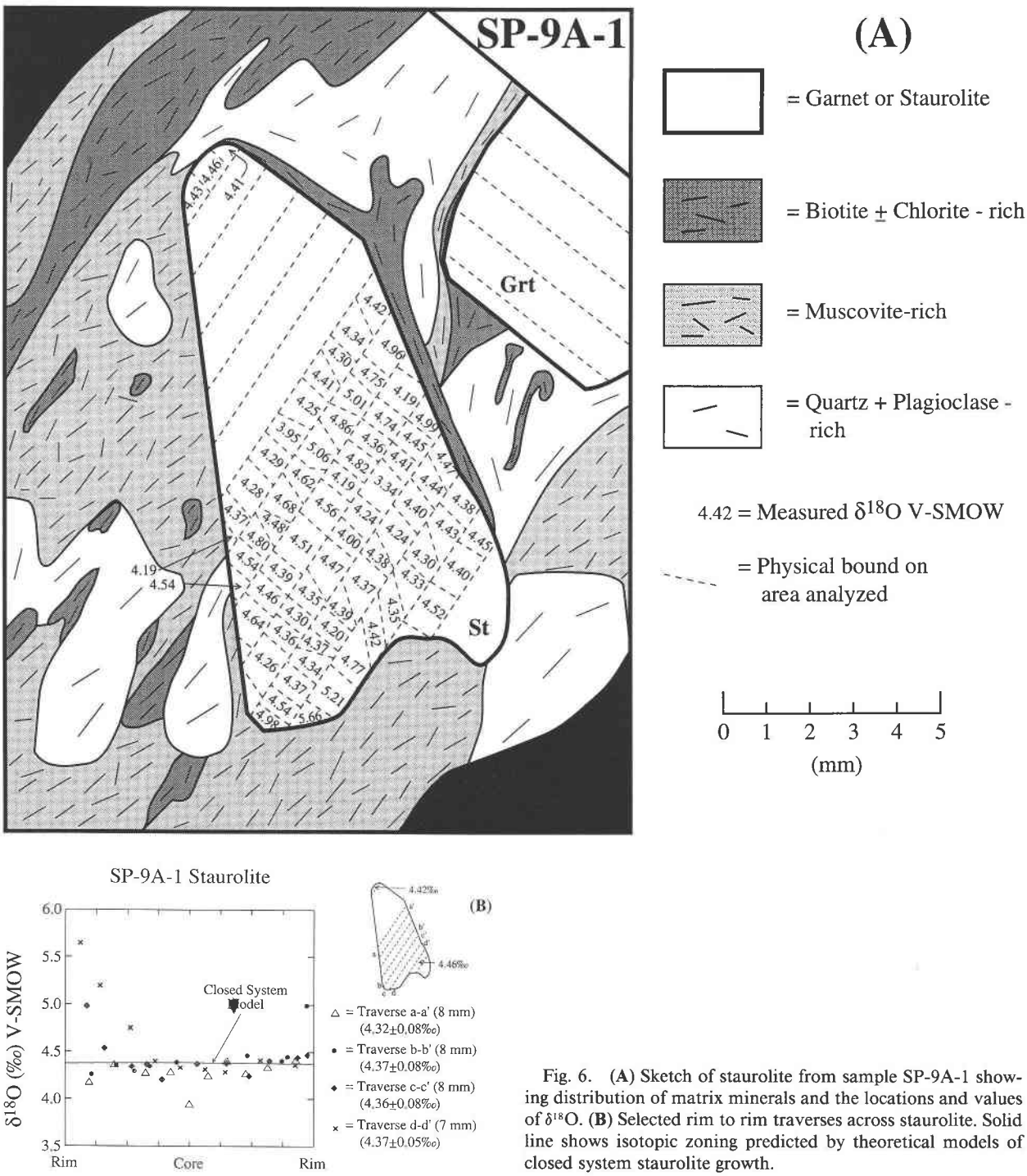

Fig. 6. **(A)** Sketch of staurolite from sample SP-9A-1 showing distribution of matrix minerals and the locations and values of $\delta^{18}O$. **(B)** Selected rim to rim traverses across staurolite. Solid line shows isotopic zoning predicted by theoretical models of closed system staurolite growth.

ical analytical precision is believed to be the result of small, nonsystematic variations in the modes of the matrix minerals. The spatial distribution of these analyses indicates that matrix isotopic composition is independent of the distance from the garnet (Fig. 5C).

Staurolite

It was initially difficult to obtain results as precise as those obtained on the garnets. Of the two traverses (21 analyses) collected prior to September 1, 1992; one shows nonsystematic variations, with a standard deviation of all analyses of ±0.2‰ (1σ), whereas the other shows two flat core-to-rim profiles (±0.12‰, 1σ) that are shifted by about 0.3‰ relative to each other. We suspect that chlorite, quartz, pyrrhotite, or ilmenite resulted in relatively poor reproducibility (±0.2‰) for the first rim-to-rim traverse and that progressive contamination of the extraction line produced an isotopic shift midway through the

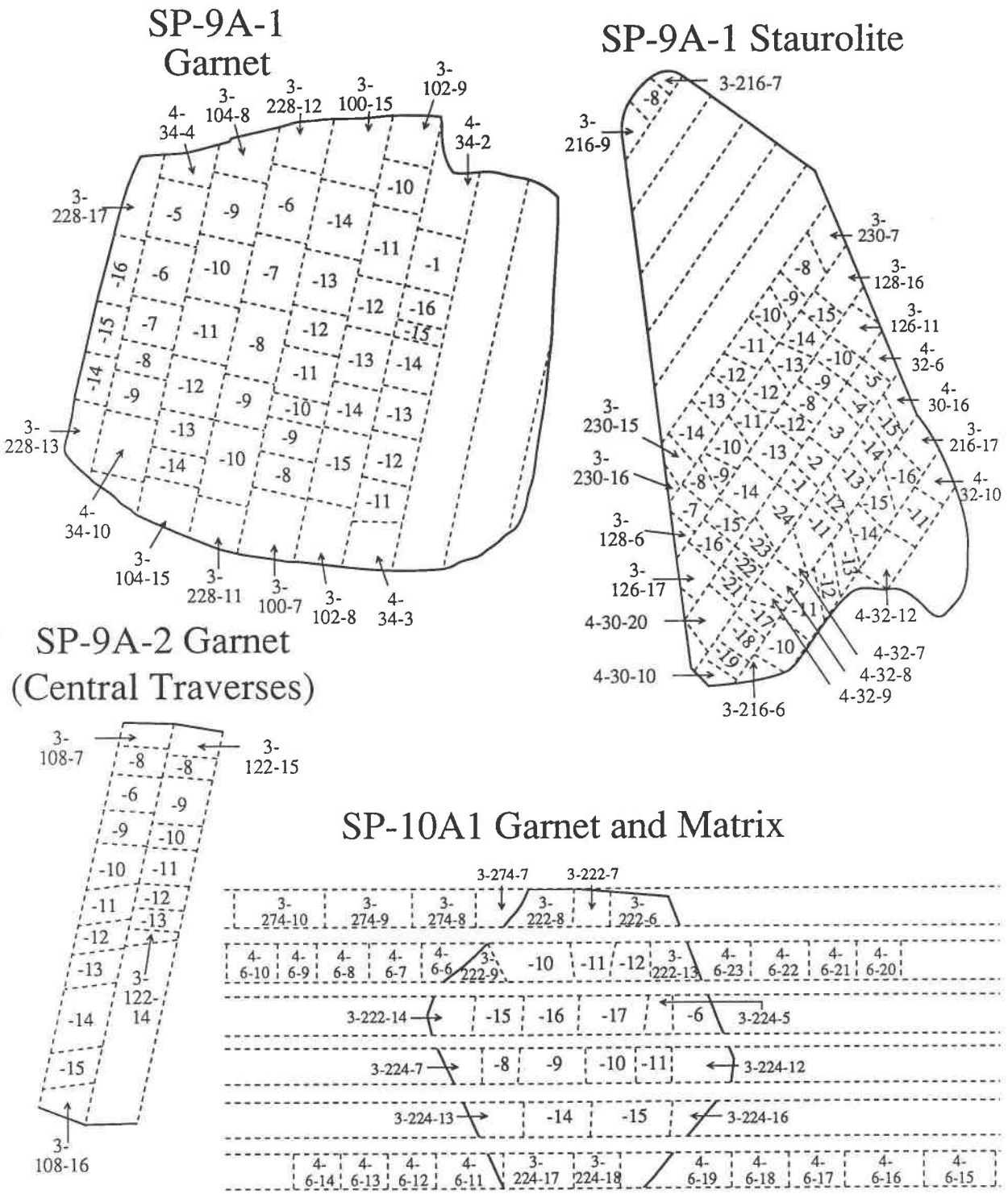

Fig. 7. Outline of garnets and staurolite studied with sample analysis locations and numbers.

second rim to rim traverse. Thus, zoning of ±0.2‰ or less was not resolvable. Although a reproducibility of ±0.2‰ is quite good for conventional staurolite analyses, it is not sufficiently precise to resolve the isotopic zoning predicted for closed system metamorphic processes (e.g., Kohn, 1993; see theoretical modeling, below). Traverses collected during September, 1992; and February, 1993; are much more internally consistent and suggest that the bulk of the staurolite is unzoned within analytical uncertainty, with a value of ~4.37 ± 0.08‰ (1σ, 40 analyses; Fig. 6B).

Five analyses collected close to the rim of the staurolite

are heavier than average, and one corner shows a dramatic increase in $\delta^{18}O$ of nearly 1.5‰ over ~2 mm (Fig. 6B). Adjacent staurolite that is slightly altered to chlorite exhibits a similar but smaller increase (~0.6‰). One other rim analysis also shows a ~0.6‰ increase in $\delta^{18}O$, but adjacent analyses do not. The matrix minerals adjacent to these rim areas are not significantly different from those adjacent to other rim areas, and although the two high $\delta^{18}O$ rims may be related to chlorite alteration processes, minor alteration elsewhere on the staurolite rim has not affected composition. Irrespective of the cause, the effect is minor and localized.

The apparent $\Delta^{18}O$ between staurolite and garnet is $\leq \sim +0.2$‰. This value is similar to that predicted by theoretical models (e.g., Richter and Hoernes, 1988). For a cooling rate of 25 °C/m.y. and with diffusivities estimated by the method of Fortier and Giletti (1989), it is unlikely that staurolite would diffusionally reequilibrate any O isotopic zonation over the scale investigated here (~0.5–1 mm).

Quartz, plagioclase, muscovite, and biotite

The number of analyses and ranges of composition observed for sample SP-9A-1 are quartz (three analyses) = 7.4–8.0‰, plagioclase (two) = 5.8–6.0‰, muscovite (four) = 4.6–4.9‰, and biotite (four) = 3.0–3.9‰. The heterogeneity observed for individual phases is greater than the analytical reproducibility, suggesting that the minerals are not homogeneously equilibrated at a centimeter scale. Relative to the garnet rim, the apparent fractionations are $\Delta^{18}O$ between quartz and garnet is +3.8 to +3.2‰, $\Delta^{18}O$ between plagioclase and garnet is +1.8 to +1.6‰, $\Delta^{18}O$ between muscovite and garnet is +0.7 to +0.4‰, and $\Delta^{18}O$ between biotite and garnet is −0.3 to −1.2‰. Based on published fractionation factors for these minerals (e.g., O'Neil and Taylor, 1967, 1969; Clayton et al., 1972; Bottinga and Javoy, 1975; Richter and Hoernes, 1988) and theoretical models of diffusional reequilibration during cooling (e.g., Eiler et al., 1992); these data are consistent with initial equilibration at peak metamorphic conditions of ~575–600 °C, with subsequent compositional heterogeneity resulting from closed-system diffusional processes.

Discussion and conclusions

Comparison of isotopic data with theoretical models

Because the *P-T* and reaction histories of samples SP-9A and SP-10A1 are well known, the compositional systematics of the garnet and staurolite allow a comparison with theoretical predictions of garnet and staurolite O isotope zonation. The theoretical model used has been described by Kohn (1993), and the interested reader is referred to that paper for more detailed information. Generally, this model is an extension of the differential thermodynamic formalism of Spear (1989) and was modified to include O isotopes as variables in addition to pressure, temperature, cation composition, and moles of oxide components. For a given bulk composition, the change of isotopic composition of each mineral can be determined as a function of the change of pressure and temperature. Consequently the closed-system isotopic zonation of a refractory phase such as garnet can be predicted as it grows during a specified *P-T* path. The matrix of the model rock is assumed to be well equilibrated over length scales that are as large or larger than the region modeled. Although the scale of O isotopic equilibration is difficult to evaluate in a coarse-grained, mineralogically heterogeneous rock, such as the metapelitic sample SP-9A, the extremely homogeneous distribution of fine-grained matrix minerals in sample SP-10A1 allows a test of the degree to which the bulk rock is equilibrated. The observed homogeneity of matrix analyses and independence of compositional trends with position around the garnet argue strongly that the assumption of matrix equilibration is reasonable.

An average pelitic bulk composition reported by Spear et al. (1990) was used to model garnet and staurolite growth in SP-9A and provides a reasonable approximation to the bulk composition. A *P-T* path and an assemblage were specified, along which the garnet and staurolite were produced as described below, and the O isotope composition of each phase was monitored along this path. Relative to quartz, we used the fractionation factors of Clayton et al. (1972; H_2O), O'Neil and Taylor (1967, 1969; plagioclase and muscovite), Bottinga and Javoy (1975; garnet and biotite), and Richter and Hoernes (1988; chlorite and staurolite). Alternate fractionation factors that shift absolute values by as much as 0.5‰ affect the magnitude of the predicted zoning trends by <0.05‰ for the garnet and by <0.01‰ for the staurolite (Kohn, 1993). Garnet and staurolite were assumed to undergo fractional crystallization, any H_2O-fluid produced was assumed to leave the system, and all other phases were assumed to be compositionally homogeneous with respect to both cations and O isotopes. Homogeneity of the isotopic composition of matrix phases may have been facilitated by the ongoing deformation reflected by rotated inclusion trails in some garnets (see Kohn et al., 1993). Models in which staurolite does not undergo fractional crystallization or in which H_2O is not lost from the system affect the predicted garnet zoning profiles by <0.02‰ (Kohn, 1993). Although these models are not strictly a closed system because of H_2O loss and fractional crystallization of garnet and staurolite, we refer to the modeled process as a closed system because no chemical interaction occurs between the rock and externally derived fluids.

Based on the petrography and *P-T* paths in Kohn et al. (1993) for metapelitic schists from the area, garnet in SP-9A was assumed to nucleate at 500 °C and 6.25 kbar in an assemblage with biotite + chlorite + muscovite + quartz + plagioclase + H_2O fluid. Inclusion or exclusion of epidote in the model affects predicted O zoning trends by only 0.04‰. On the basis of the paths in Figure 2, pressure and temperature were increased by 0.75 kbar and 75 °C, respectively, at which point staurolite was assumed to enter the assemblage. Temperature was then

increased isobarically for another 3 °C, so that approximately half the remaining chlorite was consumed, and staurolite grew. Garnet consumption occurs over this isobaric segment. Models were also constructed to determine bounds on the maximum and minimum prograde zoning possible in garnet and correspond, respectively, to (1) maximum growth of garnet from 495 to 600 °C, followed by minimum staurolite growth over a temperature increase of 3 °C, and (2) minimum growth of garnet from 530 to 575 °C, followed by maximum staurolite growth over a temperature increase of 6 °C. In this last model, chlorite is completely consumed by the staurolite-forming reaction. These ranges are consistent with the observed range of *P-T* paths estimated from metapelitic garnets and the petrography of the sample. The assumption that garnet grew within a staurolite-absent assemblage is consistent with the assumptions used in calculating the *P-T* paths (Kohn et al., 1993); and so there is the best possible internal consistency between the *P-T* path determinations and isotope models.

Garnet in amphibolitic sample SP-10A1 was assumed to nucleate and grow in the assemblage garnet (mode = 0%) + chlorite (5%) + biotite (2%) + hornblende (30%) + cummingtonite (23%) + quartz (15%) + plagioclase (25%) + H_2O fluid (0.1%) over a temperature increase of 20 °C and a pressure decrease of 1.5 kbar. The procedure described by Richter and Hoernes (1988) was used to estimate isotopic fractionation factors for hornblende and cummingtonite. For the independently estimated modes and fractionations, the predicted matrix composition of the rock is 3.67‰, in good agreement with the measured value of 3.70 ± 0.03‰ (1σ uncertainty in the mean value). If Fe_2O_3 is ignored as a system component, then the minimum zoning in garnet occurs; if Fe_2O_3 is included, then the maximum zoning is produced (Fig. 5B). The same assemblage and chemical system (with Fe_2O_3) were used to determine the *P-T* path (Kohn et al., 1993).

Predicted stable isotope profiles are plotted in Figures 4B, 5B, and 6B with the measured data and show an excellent correspondence of models and data. Predictions of the core to rim isotopic zoning in the metapelitic garnet and staurolite that are most consistent with the mineral growth are approximately +0.5 and −0.05‰, respectively, and for the amphibolitic garnet the prediction is +0.02‰. Uncertainties in the *P-T* path, the bulk compositions of the rocks, and the fractionation factors lead to a combined uncertainty in the predicted trends of approximately ±0.15 (SP-9A garnet), ±0.02 (SP-9A staurolite), and ±0.03‰ (SP-10A1 garnet), respectively (1σ; Kohn, 1993). The data and models show that there is no isotopic evidence that either rock was infiltrated by a fluid with a disequilibrium O isotope signature.

As described by Kohn (1993), bulk compositional differences and variations in assemblage can lead to distinctly different predicted mineral isotopic trends for different rocks. The most important factors are the temperature dependence of the isotopic fractionation between the whole rock and the garnet ($\Delta_{WR\text{-}Grt}$) and the effect of net transfer reactions on $\Delta_{WR\text{-}Grt}$. For most rocks, $\Delta_{WR\text{-}Grt}$ and its temperature dependence are correlated, so that the greater $\Delta_{WR\text{-}Grt}$, the greater its temperature dependence. For rocks in which $\Delta_{WR\text{-}Grt}$ and its temperature dependence are small, any zoning in garnets is minimized. If $\Delta_{WR\text{-}Grt}$ and its temperature dependence are large, then garnet composition is more strongly dependent on changes of temperature, and larger isotopic zonation can be produced. For mineral assemblages in which nearly discontinuous reactions are possible, the temperature dependence of $\Delta_{WR\text{-}Grt}$ can be less than the variation of $\Delta_{WR\text{-}Grt}$ caused by the changing mineral content of the rock. Mineral $\delta^{18}O$ compositions can then become strong functions of pressure as well as temperature, although typically a reacting phase is completely consumed before garnet rim isotopic composition changes by $>\sim$0.25‰. For most continuous reactions, the temperature dependence of $\Delta_{WR\text{-}Grt}$ controls the mineral isotopic systematics.

In amphibolite facies metabasites, $\Delta_{WR\text{-}Grt}$ and its temperature dependence are small, and no discontinuous reactions occur. Therefore, isotopic zoning in garnets from metabasites is insensitive to the *P-T* path, and the isotopic zoning predicted for such garnets will be $<\sim$0.2‰. For example, even if the garnet in the SP-10A1 metabasite grew over an interval of 100 °C in a closed system, its predicted isotopic zonation would not exceed 0.2‰. This behavior clearly indicates that garnets in metabasites should be especially sensitive monitors of fluid infiltration.

In contrast, in metapelites $\Delta_{WR\text{-}Grt}$ is typically several per mil, the temperature dependence of $\Delta_{WR\text{-}Grt}$ is larger, and there are several assemblages in which nearly discontinuous reactions can occur. As a result, garnet zoning in pelitic bulk compositions is more sensitive to the reaction history and *P-T* evolution, and isotopic trends and absolute changes of garnet $\delta^{18}O$ can be expected to show more variety. For assemblages in which nearly discontinuous reactions do not occur, garnet isotopic composition is a moderately strong function of temperature (0.1‰ per 10–20 °C), but not of pressure (0.01‰/kbar).

For the garnets in the SP-9A metapelite, each closed-system scenario that is consistent with the reaction and *P-T* histories results in prograde isotopic zoning of between 0.2 and 0.75‰, and the garnets have higher $\delta^{18}O$ towards the rim. The observed zonation of ~0.5‰ supports a garnet-growth temperature interval of ~75 °C. In general, larger or smaller increases of $\delta^{18}O$ could have occurred if the garnets had grown over a larger or smaller change of temperature. Compositional zoning in which garnets have progressively lower $\delta^{18}O$ toward the rim is also possible in closed systems but will usually only occur if garnet is produced on cooling (e.g., Kohn and Valley, 1993a; 1993b). In the metapelitic rock studied, it is evident that heating accompanied garnet production. The uncertainty of the change of temperature rather than pressure largely causes the uncertainty in the predicted isotopic growth zonation of the metapelitic garnets.

Some of the isotopic trends for different SP-9A and SP-10A1 assemblages are illustrated in Figure 8. In the lower

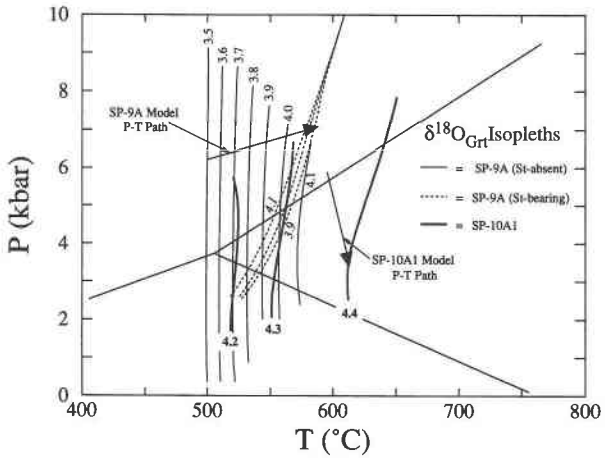

Fig. 8. Isopleths of $\delta^{18}O$ for garnet in three assemblages. SP-9A metapelitic assemblages are represented by thin lines (early staurolite absent) and dashed lines (staurolite present). Thick lines are for the SP-10A1 metabasite assemblage. Reference *P-T* conditions and compositions are from rim data for the two samples. Isotopic compositions are not necessarily relevant for *P-T* conditions far removed from the *P-T* path, and isopleths have been extended over a range of *P-T* conditions only to illustrate orientations and spacings. See text for discussion.

temperature assemblage of SP-9A, that does not contain staurolite, garnet compositional isopleths are nearly vertical and have a spacing of ~0.1‰/10 °C. The continuous reaction, chlorite + quartz = garnet + H_2O, exerts little influence on the isotopic systematics of the garnet, and it is the temperature dependence of $\Delta_{WR\text{-}Grt}$ that controls isotopic composition. In the higher temperature assemblage of SP-9A that contains staurolite, a nearly discontinuous reaction can occur: garnet + chlorite + muscovite = biotite + staurolite + H_2O. Isopleths are much more closely spaced (~0.1‰ per 2–3 °C at 7 kbar), but all chlorite will be consumed within ~6 °C, leading to a maximum change of garnet rim composition of ~0.2‰. The isopleths are also more dependent on pressure and show a decrease in garnet $\delta^{18}O$ with increasing temperature. This indicates that the mass balance of the reaction is more important in this assemblage than the temperature dependence of fractionation factors. In the SP-10A1 metabasite assemblage, there are no discontinuous reactions, and $\Delta_{WR\text{-}Grt}$ and its temperature dependence are small because of the abundance of amphibole and the paucity of quartz in the rock. As a result, garnet compositional isopleths are widely spaced, and isotopic compositions are insensitive to the *P-T* path.

Petrologic implications

The inferred isotopic bulk composition of the metapelitic rock, as indicated by the measured mineral compositions (~6.6‰), has a lower $\delta^{18}O$ than is typically assumed for metapelites and paragneisses (~12–17‰; e.g., data in Garlick and Epstein, 1967; Shieh and Taylor, 1969; Shieh and Schwarz, 1974; Wickham and Taylor, 1985). This low whole-rock $\delta^{18}O$ could imply large fluid fluxes sometime before or during metamorphism. However, the depositional origin of the metapelitic rock is unclear, and it could have had a large component of low $\delta^{18}O$ volcaniclastic material. The metapelitic rock also experienced an extremely complex geologic history prior to amphibolite-facies metamorphism, including Paleozoic lowest greenschist facies metamorphism associated with accretionary wedge formation, as well as intrusion of felsic plutons and mafic dikes during extension in the Jurassic. It is therefore unlikely that the temporal and compositional evolution of the early low-grade fluid-rock interaction is recorded.

Nonetheless, the close correspondence between theory and measurement strongly suggests that higher grade metamorphic processes can be quantitatively evaluated, and that the model of O isotopic changes described by Kohn (1993) can faithfully represent regional amphibolite facies metamorphism. The assumptions of homogeneous equilibration of matrix minerals, except for garnet and staurolite, the fractional crystallization of garnet to produce prograde O isotope zoning, and the preservation of isotopic zoning in garnet at middle- to upper-amphibolite-grade metamorphic conditions are all supported by the observed compositional trends in the garnets and staurolite and by the matrix compositions in the amphibolite. Similarly, the fact that a closed-system model reproduces the isotopic evolution of the metamorphic porphyroblasts further suggests that significant fluxing by an isotopic disequilibrium fluid did not occur during the growth of garnet and staurolite.

Limits can be placed on the fluxes of isotopic disequilibrium fluid that are consistent with the observed isotopic zonation and the theoretical model for garnet growth. Differences between closed-system models and measured isotopic zoning of >0.5 and 0.2‰ would be readily recognized in garnets from the metapelite and amphibolite, respectively. If fluid-rock ratios are considered on the basis of a simple zero-dimensional model of fluid flow, and if the fluid is assumed to be 1‰ out of equilibrium, then a fluid-rock molar ratio of 1.0 produces a shift of 0.5‰. If the fluid is 10‰ out of equilibrium then the same shift is produced with a fluid-rock molar ratio of only 0.1. If the model of Dipple and Ferry (1992) is used, and a length scale of 1 km for the flow path is assumed (based on the distance to the nearest major lithologic contact), then fluxes on the order of 5×10^3 moles of H_2O per square centimeter of rock would produce shifts of 0.5‰ or greater and would be detectable.

The close correspondence between the models and measurements gives us confidence that fluid-rock interactions during amphibolite facies metamorphism can be quantitatively evaluated in the future because deviations of isotopic zoning from closed-system predictions will be identifiable and interpretable. This study demonstrates the utility of the microanalytical isotopic approach for interpreting metamorphic processes.

Acknowledgments

J. Eiler and L. Baumgartner are thanked for valuable discussions, and B. Dutrow, J. Grambling, R. Gregory, and T. Labotka are thanked for their reviews. This work was funded by NSF grant EAR-91-05709 to J.W.V. and an NSF postdoctoral fellowship to M.J.K.

References cited

Bottinga, Y., and Javoy, M. (1975) Oxygen isotope partitioning among the minerals in igneous and metamorphic rocks. Reviews in Geophysics and Space Physics, 13, 401–418.

Chamberlain, C.P., and Conrad, M.E. (1991) Oxygen isotope zoning in garnet. Science, 254, 403–406.

Clayton, R.N., O'Neil, J.R., and Mayeda, T.K. (1972) Oxygen isotope exchange between quartz and water. Journal of Geophysical Research, 77, 3057–3067.

Conrad, M., and Chamberlain, C.P. (1992) Laser-based, in situ measurements of fine-scale variations in the $\delta^{18}O$ values of hydrothermal quartz. Geology, 20, 812–816.

Crowe, D.E., Valley, J.W., and Baker, K. (1990) Microanalysis of sulfur-isotope ratios and zonation by laser microprobe. Geochimica et Cosmochimica Acta, 54, 2075–2092.

Dalziel, I.W.D., and Brown, R. (1989) Andean core complex evolution related to marginal basin collapse: Implications for Cordillera tectonics. Geology, 17, 699–703.

Dipple, G.M., and Ferry, J.M. (1992) Fluid flow and stable isotopic alteration in rocks at elevated temperatures with applications to metamorphism. Geochimica et Cosmochimica Acta, 56, 3539–3550.

Eiler, J.M., Baumgartner, L.P., and Valley, J.W. (1992) Intercrystalline stable isotope diffusion: A fast grain boundary model. Contributions to Mineralogy and Petrology, 112, 543–557.

Elsenheimer, D., and Valley, J.W. (1992) In situ oxygen isotope analysis of feldspar and quartz by Nd:YAG laser microprobe. Chemical Geology, 101, 21–42.

——— (1993) Sub-millimeter scale zonation of $\delta^{18}O$ in quartz and feldspar, Isle of Skye, Scotland. Geochimica et Cosmochimica Acta, 57, in press.

Fortier, S.M., and Giletti, B.J. (1989) An empirical model for predicting diffusion coefficients in silicate minerals. Science, 245, 1481–1484.

Garlick, G.D., and Epstein, S. (1967) Oxygen isotope ratios in coexisting minerals of regionally metamorphosed rocks. Geochimica et Cosmochimica Acta, 31, 181–214.

Kirschner, D.L., Sharp, Z.D., and Teyssier, C. (1993) Vein growth mechanisms and fluid sources revealed by oxygen isotope laser microprobe. Geology, 21, 85–88.

Kohn, M.J. (1991) Studies of the metamorphism in west-central New Hampshire, U.S.A. and Tierra del Fuego, Chile. Ph.D. thesis, Rensselaer Polytechnic Institute, Troy, New York.

——— (1993) Modeling of prograde mineral $\delta^{18}O$ changes in metamorphic systems. Contributions to Mineralogy and Petrology, 113, 249–261.

Kohn, M.J., and Valley, J.W. (1993a) Disparate patterns of oxygen isotope zonation in garnet: All products of closed system metamorphism. European Union of Geosciences, Terra Abstracts, 5, 373.

——— (1993b) High-T fluids in the Fall Mountain nappe, southwestern New Hampshire: Infiltration vs. anatexis (abs.). Eos, 74, 332.

Kohn, M.J., Spear, F.S., and Dalziel, I.W.D. (1991) Rapid cooling following exhumation in the Cordillera Darwin metamorphic complex, Tierra del Fuego, Chile. Geological Society of America Abstracts with Programs, 23, A134.

——— (1993) Metamorphic P-T paths from Cordillera Darwin, a core complex in Tierra del Fuego, Chile. Journal of Petrology, 34, in press.

Matthews, A., Goldsmith, J.R., and Clayton, R.N. (1983) Oxygen isotope fractionation between zoisite and water. Geochimica et Cosmochimica Acta, 47, 645–654.

Nabelek, P.L. (1991) Stable isotope monitors. In Mineralogical Society of America Reviews in Mineralogy, 26, 395–435.

Nelson, E.P., Dalziel, I.W.D., and Milnes, A.G. (1980) Structural geology of the Cordillera Darwin: Collisional-style orogenesis in the southernmost Chilean Andes. Eclogae Geologicae Helvetiae, 73, 727–751.

O'Neil, J.R., and Taylor, H.P., Jr. (1967) The oxygen isotope and cation exchange chemistry of feldspars. American Mineralogist, 52, 1414–1437.

——— (1969) Oxygen isotope equilibrium between muscovite and water. Journal of Geophysical Research, 74, 6012–6022.

Richter, R., and Hoernes, S. (1988) The application of the increment method in comparison with experimentally derived and calculated O-isotope fractionations. Chemie der Erde, 48, 1–18.

Rumble, D., III (1982) Stable isotope fractionation during metamorphic devolatilization reactions. In Mineralogical Society of America Reviews in Mineralogy, 10, 327–353.

Sharp, Z. (1990) A laser-based microanalytical method for the *in situ* determination of oxygen isotope ratios of silicates and oxides. Geochimica et Cosmochimica Acta, 54, 1353–1357.

——— (1992) In situ laser microprobe techniques for stable isotope analysis. Chemical Geology, 101, 3–19.

Shieh, Y.-N., and Schwarz, H.P. (1974) Oxygen isotope studies of granite and migmatite, Grenville province of Ontario, Canada. Geochimica et Cosmochimica Acta, 38, 21–45.

Shieh, Y.-N., and Taylor, H.P., Jr. (1969) Oxygen and hydrogen isotope studies of contact metamorphism in the Santa Rosa Range, Nevada and other areas. Contributions of Mineralogy and Petrology, 20, 306–356.

Spear, F.S. (1989) Petrologic determination of metamorphic pressure-temperature-time paths. In F.S. Spear and S.M. Peacock, Eds., Metamorphic pressure-temperature-time paths, short course in geology, p. 1–55. American Geophysical Union, Washington, DC.

Spear, F.S., Kohn, M.J., Florence, F., and Menard, T. (1990) A model for garnet and plagioclase growth in pelitic schists: Implications for thermobarometry and P-T path determinations. Journal of Metamorphic Geology, 8, 683–696.

Valley, J.W. (1986) Stable isotope geochemistry of metamorphic rocks. In Mineralogical Society of America Reviews in Mineralogy, 16, 445–489.

Wickham, S.M., and Taylor, H.P., Jr. (1985) Stable isotopic evidence for large-scale seawater infiltration in a regional metamorphic terrane. The Trois Seigneurs Massif, Pyrenees, France. Contributions to Mineralogy and Petrology, 91, 122–137.

Manuscript received November 4, 1992
Manuscript accepted May 26, 1993

Note added in proof

More recent analysis of standards allows a refinement of correction procedures for laser probe analysis. A total of 371 analyses of the UW Gore Mountain garnet standard was made by four analysts between September 1, 1992, and July 15, 1993; the uncorrected value of $\delta^{18}O$ is 6.03 ± 0.13‰ (ls), virtually identical to the value reported here of 5.99 ± 0.07‰ for 79 analyses. The correction of these raw data to the SMOW scale is based on comparison with 17 laser analyses of NBS28, seven from before cleaning of the extraction line in September, 1992. Since September, the day-to-day variations have been typically <0.1‰, and the differences between NBS28 and UW Gore Mountain garnet average 3.39‰ for 47 new quartz analyses (NBS28 = 9.42 ± 0.13‰). Thus, the corrections made in this paper may be uniformly ~0.2‰ too large, and analyses since September suggest corrections of 0.2 ± 0.1‰.